Volume 10, Issue 3, 2020, 5369 - 5375 ISSN 2069-5837
Biointerface Research in Applied Chemistry
www.BiointerfaceResearch.com
https://doi.org/10.33263/BRIAC103.369375
Original Research Article Open Access Journal
Received: 28.01.2020 / Revised: 03.03.2020 / Accepted: 05.03.2020 / Published on-line: 09.03.2020

Effective adsorptive removal of azodyes on synthesized copper oxide nanoparticles

Madiha Batool [1], Shazia Khurshid [1], Zahid Muhammad Qureshi [1], Walid Mohamed Daoush [2, 3] *, Farwa Hashmi [4], Nida Mehboob [4]

[1]Department of Chemistry, Government College University (GCU), Lahore, Pakistan
[2]Department of Production Technology, Faculty of Industrial Education, Helwan University, Cairo, Egypt
[3]Department of Chemistry, College of Science, Imam Mohammad ibn Saud Islamic University (IMSIU), Al Riyadh, KSA
[4]Lahore College for Women University, Lahore, Pakistan

*corresponding author e-mail address: ***wmdaoush@imamu.edu.sa*** | Scopus ID 35609965600

ABSTRACT

Copper oxide nanoparticles were synthesized by using *Camellia Sinensis* leaves extract as a reducing and capping agent of the copper ions in solutions and its azodyes adsorptive efficiency were studied. The produced copper oxide nanoparticles were subsequently characterized by SEM, TEM, XRD, FTIR, and UV spectrophotometer for investigating its particle shape, size, crystalline phase and chemical composition. The particle size of the prepared copper oxide nanoparticle was calculated from the XRD data by using the Scherrer equation was found 17.26 nm. However, the median particle size calculated from the SEM and TEM image analysis was found 25~85 nm of tetragonal particle shape. UV spectrum was obtained with maximum absorption peak at 280 nm. The FTIR spectrum indicated -OH, -C=C- and -C-H functional groups, which is due to the presence of the stabilized layer of the *Camellia Sinensis* leaf extract which is binded with the prepared copper oxide nanoparticles. The produced copper oxide nanoparticles were used for studying the degradation of Congo red and Malachite green azodies. Different parameters were studied to optimize the reaction conditions. Kinetic models of Langmuir, Freundlich and Elovich models were also applied. The degradation percent of the investigated azodyes on the surface of the produced copper oxide nanoparticles in aqueous solutions was observed between 70-75%.

Keywords: *Camellia Sinensis; Copper oxide nanoparticles; Green synthesis; Congo red; Malachite green; Adsorption kinetics.*

1. INTRODUCTION

Industrial wastes contaminated by coloring dyes having a large number of organics, which are hazard to the environment by their capability to increase mutagenic effects [1, 2]. Malachite green dye is extensively used in industry and it is a water soluble cationic azodye, belongs to the class of triphenyl methane [3]. Congo Red dye is another water-soluble carcinogenic and xenobiotic azodye used in fabrication of textile and paper industry [4-7]. Table 1 lists the different properties and toxicity of the Malachite green and the Congo red azodyes.

Table 1. Properties and toxicity of Malachite green and Congo red azodyes [4-7].

Properties	Malachite green	Congo red
Molecular mass	364.91g/mol	696.68g/mol
Molecular formula	$C_{23}H_{25}N_2$	$C_{32}H_{22}N_6Na_2O_6S_2$
Physical state	Green powder	Red powder
Toxic effect	Skin, eyes irritation and lung adenomas	Neurotoxic and pancreatic toxicity
Stability	stable	stable
Melting point	164	360
LD_{50}	80mg/kg	296mg/kg
Water solubility	Soluble	Soluble

There are numerous methods to discard azodyes from the colored effluents to minimize their impacts. Adsorption is one of the unique technological methods for azodye degradation [8]. Synthesized metal oxide nanoparticles can be applied for the catalytic degradation of azodyes. It is an economical method as compared to other reported methods in the literature. This adsorption effect of pure metal oxides nanoparticles can be contributed to the ratio between the large surface area of the active sites and the small particle size [9]. However, the adsorption activity of these metal oxides nanoparticles is depending on the synthesis method, particle size, particle shape, particle dispersion, and the nature of supporting material.

The biosynthesis of metal oxide nanoparticles like copper oxide nanoparticles, has been considered as a cost-effective and environmentally friendly alternative to the physical and chemical methods. Plant-mediated synthesis of metal oxides nanoparticles is one of the green chemistry approaches that consider plants extracts as stabilizing agents of metal oxide nanoparticles used in different applications in nanotechnology [10-12].

Copper oxide nanoparticles act as effective catalyst for dyes adsorption and removal leads to the degredation processes [13]. Most probably, copper oxide has low cost and can be recently used as a unique adsorbent of azodyes and its nanoparticles have efficiency of azodyes removal from industrial waste water [14, 15]. Copper oxide nanoparticles have been synthesized by using leaf extract of *Camellia Sinensis*. *Camellia synesis* leaves extracts have several types of organic compounds such as 30 wt.% of polyphenols, 15 wt.% of proteins, 4 wt. % of amino acids, 7wt. % of carbohydrates, 7 wt.% of lipids, 10 wt. % of Vitamin C and D. in addition; catechins which included -OH active groups used in solutions as a reducing agent of copper ions to copper metal [16].

The Camellia *synesis leaves* extract can be used as reducing and capping agents during the synthesis of metal nanoparticle from its soluble salts [17-21]. The phenolic content in plants extract which was biodegradable and can be catalyzed the synthesis of copper oxide nanoparticles acting as capping and reducing agent [22-24]. Table 2 lists the main active components

of different types of plants which can be used as reducing and stabilizing agents of metal oxide nanoparticles.

The main aim of this work is, to synthesize copper oxide nanoparticles using *camellia sinensis* leaves extract as a reducing, capping and stabilizing agent. The crystalline structure, chemical composition, particle size, shape and morphology were investigated by X-ray diffraction (XRD), Fourier transform infrared (FTIR) spectroscopy, UV spectroscopy, scanning electron microscopy (SEM) and transmission electron microscopy (TEM). The catalytic degradation efficiency of the prepared copper oxide nanoparticles was investigated by determining the degradation of Malachite green and Congo red azodyes in aqueous solution. The reaction parameters like pH, temperature and removal time and its effect on the dye degradation were studied. The kinetic models (pseudo-second order, Langmuir, Freundlich and Elovich) were studied to determine the mechanism of the dye degradation.

Table 2. Fabrication of metal oxide nanoparticles by using active components of different plant species.

Plant species	Metal oxide NPs	Active component	Size, nm	References
Aloe barbadensis	Cu_4O_3	Phenols and proteins	30-60	13
Azadirachta indica	Cu_4O_3	Flavanones or terpenoids	~28–30	12
Phyllanthus Amarus	CuO	Not mention	50	9
Hibiscus rosasinensis	Cu_4O_3	Phenolic compound	30-50	3
Aloe barbadensis	CuO	Carbonyl groups	15 -30	4
Gum karaya	CuO	Carbohydrates, proteins	7.8 ± 2.3	25
Arachis hypogaea	Cu_2O	Phenolic compound	37	19

2. MATERIALS AND METHODS

2.1. Materials.

All chemicals used were of analytical grade and pure. The chemicals used for the preparation of copper nanoparticles include copper sulfate pentahydrate ($CuSO_4.5H_2O$) purchased from Sigma Aldrich Co. LTD. The *Camellia Sinensis* leaves were supplied from the botanical garden of the Government College University (GCU), Lahore, Pakistan.

2.2. Preparation of the *Camellia Sinensis* leaves extract.

Camellia Sinensis leaves of 30g were collected and then washed with distilled water. The cleaned leaves were dried and grounded. 100 ml of deionized water was added to the obtained powder of the grounded leaves. The obtained solution was boiled for 10 minutes and subsequently stored at low temperature after filtration [26].

2.3. Preparation of copper oxide nanoparticles.

A copper sulfate pentahydrate solution of 50 ml was added and stirred with 5ml of the obtained ***Camellia Sinensis*** leaves extract by using Magnetic stirrer. The reaction is started when the color of the solution changed from green to pale yellow then finally to dark brown. Whenever the reaction was completed, the solution was centrifuged for 20 mints at speed of 1000 rpm. After removal of supernatant, the obtained nanoparticles was washed with ethanol then dried. The obtained nanoparticles was Calcination for one hour at 500^{o}C. The obtained black colored nanoparticles were stored for characterization [26-30].

2.4. Characterization of the copper oxide nanoparticles.

Scanning electron microscope (SEM) supported with EDS unit, transmission electron microscope (TEM), X-ray diffractometer (XRD), UV spectrophotometer and Fourier transform infrared (FTIR) spectrophotometer were used in order to characterize the particle size, shape, crystalline structure and chemical composition of the obtained copper oxide nanoparticles.

2.5. Preparation of standard solution from the dye.

Two separate stock solutions of Malachite green and Congo red azodyes of concentration 1000 ppm in a liter of distilled water were prepared. The obtained stock solutions were used to prepare different solutions with different concentrations of the investigated azodyes. The stock solutions were diluted to prepare three different solutions contains 150, 200, 250 of the investigated azodyes separately. The azodyes removal or degradation efficiency using the copper oxide nanoparticles was evaluated by calculating the dye decolorization percentage according to equation (1) as follows;

$$\text{Decolorization \% of the dye} = A\text{-}B\ /A\times 100 \quad (1)$$

Where A and B are absorbance of the investigated azodye solution in the presence of the copper oxide nanoparticles and in the absence of the copper oxide nanoparticles respectively**.**

2.6. Dye degradation and Kinetic studies.

Exact 50 micro-liters of hydrogen peroxide H_2O_2 solution (200 µmole) was added as an oxidizing agent to release the peroxide free radicals. Four samples with different compositions were prepared to study the different reaction parameters of the degradation of the investigated azodye. Two samples for Malachite green and another two samples for Congo red dye with and without using hydrogen peroxide as a reducing agent were prepared. The effect of removal time, temperatures and pH were studied to optimize the reaction conditions. The initial concentration of the produced copper oxide nanoparticles adsorbent was chosen in the range between 20-250 mg/L. The concentrations of the Congo red and the Malachite green dyes in aqueous solutions were measured by using the UV–VIS spectrophotometry technique. On the other hand, the adsorption kinetics of the investigated azodye were carried out under the selected optimum operating conditions. A solution prepared by dissolving and stirring 20 mg of the produced copper oxide adsorbent nanoparticle in 50 ml solution contains 10 ppm of the investigated dyes was used to study the adsorption kinetics of the dyes on the surface of the prepared copper oxide nanoparticles.

3. RESULTS

3.1. Particle size, morphology and crystal structure.

During the reduction of the copper sulphate salt by the *Camellia sinensis* leaves extract, the green color of the solution turned into dark brownish color indicating the formation of copper oxide nanoparticles. The obtained nanoparticles were investigated to determined its particle size, shape, morphology and crystalline

structure. The median particle size, shape and morphology of the produced copper oxide nanoparticle were investigated by the SEM and TEM as shown in Figure 1 (a-c). It was observed from the results of the calculated median particle size that; the particle size is between 25 nm and 500 nm. It was also observed from the result that; the particles have tetragonal shape and some of the particles are agglomerated to form nanoclusters. The EDS analysis of the produced nanoparticles revealed that the particles are mainly composed of copper and oxygen. In addition; some elemental inclusions detected which is formed from the chemical solution of the leaves extract during the preparation method.

The X-ray diffraction pattern of the produced copper oxide nanoparticles was examined by using the X-ray diffractometer. It was observed from the XRD pattern as shown in Figure 1(d) that; the produced copper oxide nanoparticles have diffraction pattern matched with the JCPDS card number (033-0480) of Cu_4O_3. The peaks which appeared at 2θ of 28.09°, 30.61°, 36.14° and 44.1 ° of the crustal planes 112, 103, 202 and 213 respectively which revealed the presence of the tetragonal crystalline structure of Cu_4O_3. However, the crystal size which was calculated by the Scherrer equation was found 17.2 nm.

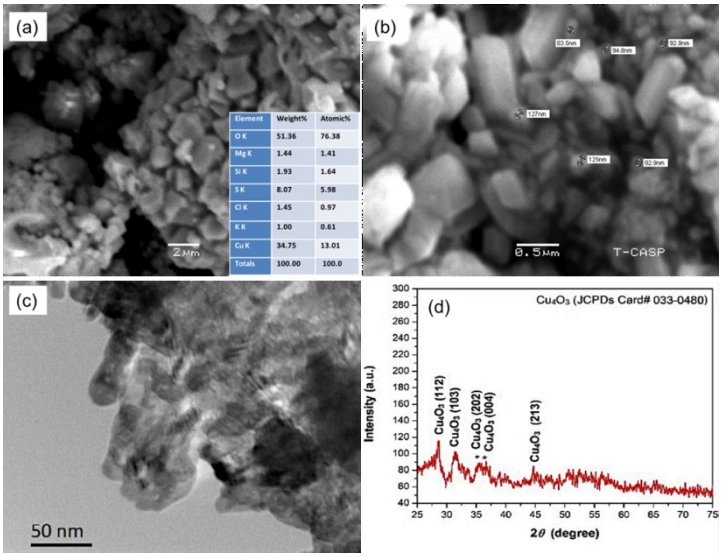

Figure 1. (a, b) SEM images with different magnifications, EDS compositional analysis, (c) TEM image and (d) XRD pattern of the produced copper oxide (Cu_4O_3) nanoparticles by using *Camellia sinensis* leaves extract as a reducing and stabilizing agent.

3.2. Ultraviolet and FTIR spectroscopy.

Figure 2 (a) shows the UV-Visible spectra of the prepared Cu_4O_3 nanoparticles. The wavelength at which the copper oxide nanoparticles can be detected is 200-400 nm. The maximum absorption peak was appeared at 280 nm which confirmed the presence of the copper oxide nanoparticles.

Figure 2 (b) presented FTIR chart of the stabilized copper oxide nanoparticles. The overall spectrum was observed in range from 500 to 4000 cm^{-1}. It was observed from the results that; the bands appeared at 3310, 2850, 1611, 1344 and 1100 cm^{-1} indicate the presence of -O-H stretching of the alcohol, the -C-H stretching of the alkene, the -C=C- stretching of aromatic ring, the bending of the -C-H bond and the Cu-O- of the Cu_4O_3 respectively.

3.3. Effect of experimental parameters on the dye degradation

3.3.1. Effect of time.

Effect of reaction removal time on the azodye degradation was studied by measuring the UV spectrum of the obtained copper oxide nanoparticles synthesized by using *Camellia Sinensis* as reducing, capping and stabilizing agent. Figure 3 shows the effect of time required for the removal of the dye. The results observed that; the maximum degradation percentage has occurred after 45 min. and the removal percentage was observed for both Malachite green and Congo red dye is between 70-75%.

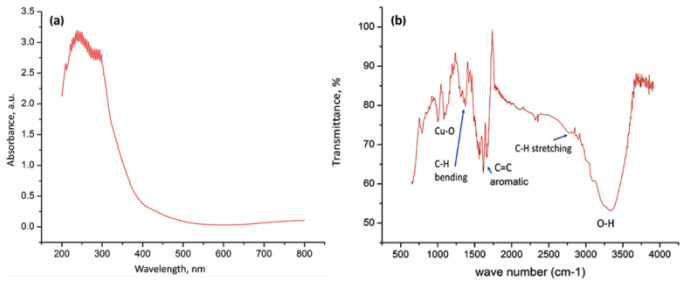

Figure 2 (a) UV-VIS spectrum and (b) FTIR chart of the produced copper oxide (Cu_4O_3) nanoparticles by using Camellia sinensis leaves extract as a reducing and stabilizing agent.

The result clearly shows the effect of removal time on the degradation of the Malachite green as well as the Congo red dyes by using the prepared Cu_4O_3 adsorbent nanoparticles in the presence and absence of the hydrogen peroxide as a reducing agent. It was observed from the results that the dye degradations were enhanced in the presence of the hydrogen peroxide reducing agent.

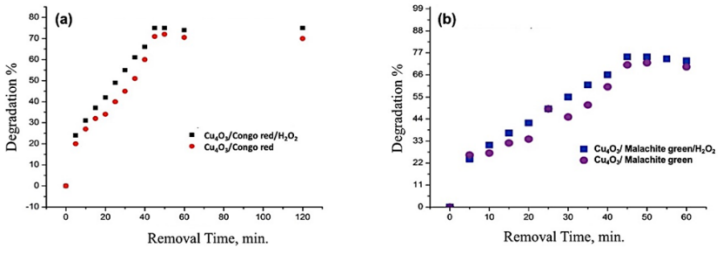

Figure 3 Relationships between the removal time and the degradation % of a) Congo red and b) Malachite green dye in the presence and absence of hydrogen peroxide reducing agent by using the Cu_4O_3 nanoparticles adsorbent.

3.3.2. Effect of pH.

Effect of pH on the removal of Congored and Malachite green azodyes by using the UV spectrophotometry was studied. The degradation % of the dyes using the copper oxide absorbent nanoparticles was experimentally performed at pH range between 2 and 14. Figure 4 shows the maximum degradation % and removal of both the Malachite green and Congo red dyes was observed at pH around 3.

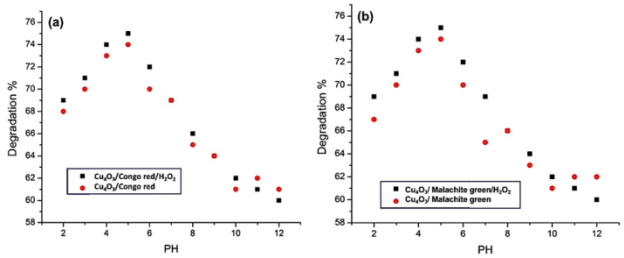

Figure 4 Effect of pH on the degradation % of a) Congo red and b) Malachite green dye in the presence and absence of hydrogen peroxide reducing agent by using the Cu_4O_3 nanoparticles adsorbent.

3.3.3. Effect of Temperature.

The effect of temperature on the degradation of the investigated dyes by using the obtained copper oxide adsorbent

nanoparticles was studied. The observed results were shown in Figure 5 indicate that; the maximum degradation % in case of the Congo red dye has occurred at 60°C. However, in case of the Malachite green dye the maximum degradation % has takes place at 70 °C.

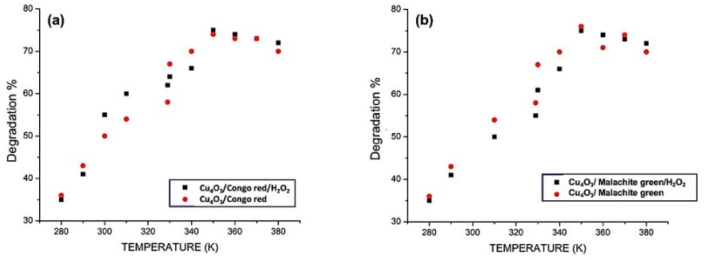

Figure 5 Effect of temperature on the degradation % of a) Congo red and b) Malachite green dye in the presence and absence of hydrogen peroxide reducing agent by using the Cu_4O_3 nanoparticles adsorbent.

3.4. Kinetics studies of the adsorption process.

The kinetic parameters are helpful for estimating the adsorption rate. It was observed from the results in Figure 6 that; the pseudo-second-order model is clearly presented the adsorption kinetics of the removal process. The results indicated a significant potential of the copper oxide nanoparticles as adsorbent for the investigated azodye removal. The straight line represented that the nanoparticles follow a pseudo-second-order kinetics rather than first order.

The plotted data proves that; the pseudo-second-order kinetics of the Congo red and the Malachite green dyes have regression coefficient (r^2) value of the values 0.997, 0.99, 0.998 and 0.989 in the presence and absence of H_2O_2 respectively. The graphical representation of the model in Figure 6 shows that the pseudo-second-order model explain the adsorption kinetics most effectively. The model can be represented by the following deferential and its corresponding integrated equation as follows;

$$\frac{dq_t}{dt} = k_1 (q_e - q_t) \quad (2)$$

$$(t/q_t) = (1/ K q_e^2) + (1/q_e) t \quad (3)$$

Where, q_t represent the amount of adsorbent at time, d_t is change in time interval, k_1 is a constant, q_e is the amount of the copper oxide nanoparticles adsorbent at equilibrium. The pseudo-second-order model considers the rate-limiting step as the formation of chemisorptive bond involving sharing of electrons between the adsorbate azodye molecules and the copper oxide nanoparticles adsorbent. If the pseudo-second order kinetics can be applicable, the plot of (t/q_t) versus t gives a linear relationship that allows to compute the q_e and K. In the present experiment, the kinetics are investigated with (C_o= 20 mg/L) at 303K with the interaction time intervals between 1 and 60 min. The obtained plots in Figure 6 between (t/q_t) versus the contact time (t) of the Malachite green and Congo red dyes decolorization represented that the model fitted the best decolorization % and also the results indicated a significant potential of the produced copper oxide nanoparticles as an adsorbent for removing the investigated azodyes.

3.5. Adsorption reaction isotherm models.

3.5.1. Langmuir isotherm model.

The Langmuir isotherm is one of the applicable expression of solute adsorption as monolayer adsorption on a surface having few numbers of identical sites. Langmuir isotherm model provides energies of adsorption by easy way. That's why the Langmuir isotherm model is selected for evaluating the adsorption capacity of the monolayer surface of the adsorbent. Adsorption process fits the Langmuir and pseudo-second order models. Langmuir isotherm or single crystal surfaces describes also the adsorption process at low, medium and multilayer coverage are also ruled out.

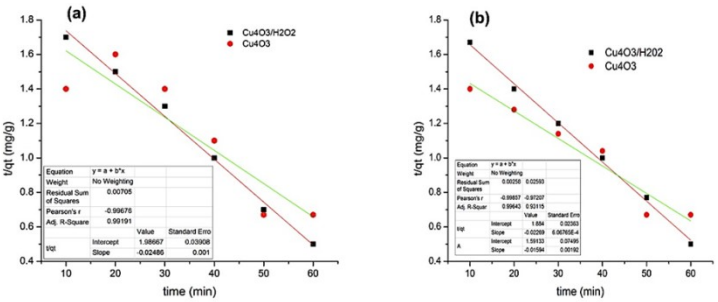

Figure 6 Pseudo-second-order kinetics of a) Congo red and b) Malachite green dye in the presence and absence of hydrogen peroxide reducing agent by using the Cu_4O_3 nanoparticles adsorbent.

Adsorbates are chemically adsorbed at a fixed number of well-defined sites, each sit can hold only one adsorbate species, all sites are energetically equivalent, there is no interaction between the adsorbate species according to this model. The Langmuir relationship can be represented by deferential as well as and its corresponding integrated equation as follows;

$$q_e/q_m = b\, C_e/ (1+bC_e) \quad (4)$$

$$C_e/q_e = 1/(K_L . q_m) + (1/q_m)\, C_e \quad (5)$$

Where q_m is, the adsorption capacity in unit mg/g and q_e is the adsorption capacity at equilibrium, K_L is the Langmuir isotherm constant which provides the binding affinity between the copper nanoparticles adsorbent (Cu_4O_3) and the investigated azodye. C_e is the equilibrium concentration of the investigated azodye. The values of isotherm q_m and constant K_L can be calculated by plotting a graph between C_e/q_e and C_e in case of the Congo red and the Malachite green azodyes as shown in Figure 7 (a, b). The characteristics of the Langmuir isotherm can be examined in terms of its equilibrium parameters and the K_L and can be calculated by the above mentioned mathematical formula.

From the ploted data between (C_e/q_e) and C_e as seen in Figure 7 (a, b), the slope $1/(bq_m)$ and the intercept (1/b) can be calculated by extrapolation. Further analysis of Langmuir equation is studied on the basis of the values of the separation factor R_L according to the following equation;

$R_L = 1/ (1+ b\, C_e)$ (where $0 < R_L < 1$ for a favorable adsorption) (6)

It was observed from the plotted data that the obtained linear isotherm has the value of $R_L < 1$. The rate constant K_L was estimated by calculating the slop and it was found to be 0.015 for Congo red dye and 0.0076 for Malachite green dye with concentration of 20 mg/l and nanoparticles adsorbent concentration of 0.25 g/l for all the obtained isotherms at 35°C. The Langmuir isotherm was drawn for the data to and the correlation coefficient R^2 values were obtained of 0.9819, 0.999 in the presence of H_2O_2 reducing agent and 0.994, 0.996 in the absence of H_2O_2 reducing agent for Congo red and Malachite green dye. The decolorization % indicating strong binding of the investigated azodyes to the surface of Cu_4O_3 nanoparticles

adsorbent [26-28]. It was observed from the results that the Langmuir adsorption model well fit the experimental data.

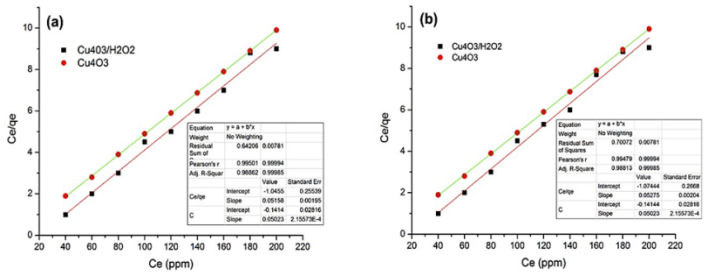

Figure 7. Langmuir model of a) Congo red and b) Malachite green dye in the presence and absence of hydrogen peroxide reducing agent by using the Cu_4O_3 nanoparticles adsorbent.

3.5.2. Freundlich Isotherm model.

Freundlich presented an empirical dye decolorization isotherm equation that can be applied in case of low and intermediate dye concentrations. The Freundlich isotherm model is suitable for the adsorption of dye on the adsorbent particles. It is easier to handle mathematically in more complex calculations. The Freundlich isotherm is given by applying the following equation;

$$q_e = K_f C_e^{n} \quad (7)$$

Where q_e is, the amount used of the investigated azodye in unit of mg/g, C_e is the equilibrium concentration of the dye, K_f in mg represents the dye decolorization capacity at the dye equilibrium concentration and n represents the dye decolorization degree of dependence at the equilibrium concentration. By applying the logarithms on both sides of equation (7), the following equation was obtained;

$$\ln q_e = \ln K_f + n \ln C_e \quad (8)$$

By drawing the Freundlich isotherm between ln C_e and ln q_e. It was observed from the results that the obtained graph between ln q_e and ln C_e shows a linear relationship as shown in Figure 8 (a, b). Also, it was revealed from the obtained Freundlich isotherm graph by linear square method of the experimental data that; a poor correlation was observed by applying the Freundlich model, which confirmed by the r^2 values 0.90, 0.93 for Congo red and Malachite green dyes in the presence and absent of H_2O_2 reducing agent respectively. Both the investigated azodyes of Congo red and Malachite green by using Cu_4O_3 nanoparticles adsorbent do not correspond to the acceptable r^2 value and the obtained value of r^2 at the experimental temperature condition (35^{o}C) is not well fitted. The n value was graphically calculated to be above 1 which represents the model is nonfitted the data. The n value of the above-mentioned equations was not satisfying the condition of ($0 < n < 1$) indicating non-favorable dye decolorization and the Langmuir model was fit the resulted data better than the Freundlich model. Also by applying the Freundlich model the adsorption activity of the produced Cu_4O_3 nanoparticles was observed not suitable for the degradation of Malachite green and Congo red azo dyes.

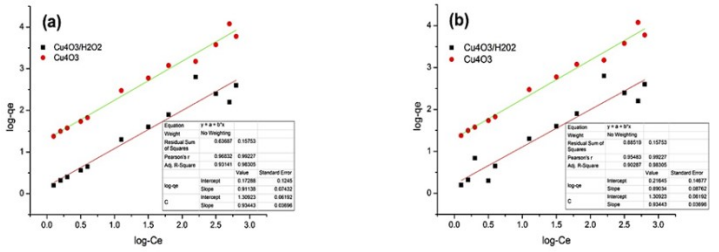

Figure 8 Freundlich model of a) Congo red and b) Malachite green dye in the presence and absence of hydrogen peroxide reducing agent by using the Cu_4O_3 nanoparticles adsorbent.

3.5.3. Elovich adsorption model.

Elovich model can be applied in adsorption reaction kinetics. It can be used to follow the mechanism of reaction. The intensity of adsorption process is a prediction of the bond energies between the investigated azodyes and the copper oxide nanoparticles adsorbent, indicating the possibility of the chemisorption (formation of chemical bonds) process rather than the physisorption (electrostatic attraction) process [31- 33]. The pseudo-second-order reaction differs with Elovich model in the type of constants. Elovich model used to study the rate constant, the pseudo-second-order half-life time and the initial rate of reaction are calculated. In Elovich model a logarithmic mathematic function are applied. This model shows a chemisorption process as in the following equation;

$$q_t = \ln(\alpha.\beta) + \ln t \quad (9)$$

The Elovich model is specified to determine the rate constants (adsorption rate and desorption rate). It relates the extensive absorptions sites and the equation of the boundary conditions gives as follows;

$$q_t = 1/\beta \ln(\alpha.\beta) + 1/\beta \ln t \quad (10)$$

Where q_t is the adsorbent amount at time t, α (mg. g $^{-1}$. min $^{-1}$) is the initial sorption rate and β (g·mg^{-1}) is related to the extent of surface coverage and the activation energy involved in the chemisorption. By applying the obtained data in equation 10, the Elovich model can be obtained as shown in Figure 9. The r^2 values of the obtained Cu_4O_3 nanoparticles adsorbent with and without using H_2O_2 reducing agent for the Congo red and Malachite green azodyes were 0.989, 0.997, 0.987, 0.988 respectively. This show that; the Elovich model is suitable to fit the data, however, it is less fitted the data than the Langmuir kinetic model. However, the Freundlich kinetic model is the least model to fit the data than the other models [27-33].

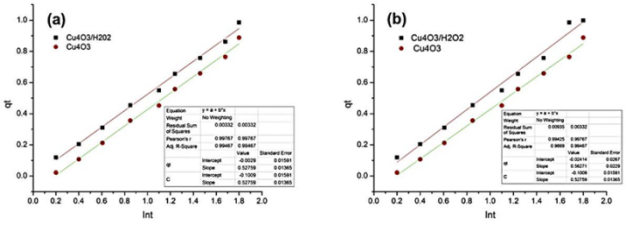

Figure 9. Elovich model of a) Congo red and b) Malachite green dye in the presence and absence of hydrogen peroxide reducing agent by using the Cu_4O_3 nanoparticles adsorbent.

4. CONCLUSIONS

This study has been carried out by using copper oxide nanoparticles synthesized via *Camellia Sinensis* leaves extract as a reducing, capping and stabilizing agent. A nanosized Cu_4O_3 particles was obtained. The UV spectrum of the obtained nanoparticles indicating an absorption peak at 280 nm which confirmed the formation of the Cu_4O_3 nanoparticles. The particle size was calculated by Scherrer equation and was about 17.26 nm. The SEM and TEM image analysis of the obtained nanoparticles

confirmed a tetragonal particle shape of the prepared Cu_4O_3 particles with average diameter of 25 ~ 85 nm. The FTIR spectra indicated different bands of -OH, -C=C-, -C-H functional groups, which is due to the presence of the *Camellia Sinensis* leaf extract layers surround and stabilized the obtained Cu_4O_3 nanoparticles in the solution. The calculated surface area of the obtained copper oxide nanoparticles was 65 m^2/g. The obtained copper oxide nanoparticles were used as bio-sorbent for the removal of Congo red and Malachite green azodyes. The degradation % of Malachite green and Congo red azodyes are in the range between 70-75% at the optimum reaction conditions. Results of different reaction parameter revealed that the optimum pH was found 3-4, removal time of 30-40 minutes and reaction temperature of 70-80^oC. The kinetic isotherm data revealed that a correlation with common adsorption isotherm equation which confirmed a chemisorption of monolayer follow the Langmuir, Elovich models with maximum capacity of 20 mg/g for Congo red and 32 mg/g for Malachite green azodyes. The reaction kinetics followed a pseudo-second order for both the investigated azodyes rather than first order. The Langmuir model fits better with linearity rather than Freundlich model predicted chemisorption. The Elovich model also has a linear fitting of the obtained data. It was expected that the copper oxide Cu_4O_3 nanoparticles keep excellent azodyes degradation potential at optimum conditions.

5. REFERENCES

1. Bahadar, H.; Maqbool, F.; Niaz, K.; Abdollahi, M. Toxicity of Nanoparticles and an Overview of Current Experimental Models. *Iranian biomedical journal* **2016**, *20*, 1-11, https://doi.org/10.7508/ibj.2016.01.001.
2. Aksu, Z. Application of biosorption for the removal of organic pollutants: a review. *Process Biochemistry* **2005**, *40*, 997-1026, https://doi.org/10.1016/j.procbio.2004.04.008
3. Xi, Y.; Hu, C.; Gao, P.; Yang, R.; He, X.; Wang, X.; Wan, B. Morphology and phase selective synthesis of CuxO (x=1, 2) nanostructures and their catalytic degradation activity. *Materials Science and Engineering: B* **2010**, *166*, 113-117, https://doi.org/10.1016/j.mseb.2009.10.008.
4. Mustafa, G.; Tahir, H.; Muhammad, S.; Nasir, A. Synthesis and characterization of cupric oxide (CuO) nanoparticles and their application for the removal of dyes. *African Journal of Biotechnology* **2013**, *12*, 6650-6660, https://doi.org/10.5897/AJB2013.13058.
5. Somasekhara Reddy, M.C.; Sivaramakrishna, L.; Varada Reddy, A. The use of an agricultural waste material, Jujuba seeds for the removal of anionic dye (Congo red) from aqueous medium. *Journal of Hazardous Materials* **2012**, *203-204*, 118-127, https://doi.org/10.1016/j.jhazmat.2011.11.083.
6. Binupriya, A.R.; Sathishkumar, M.; Swaminathan, K.; Kuz, C.S.; Yun, S.E. Comparative studies on removal of Congo red by native and modified mycelial pellets of Trametes versicolor in various reactor modes. *Bioresource Technology* **2008**, *99*, 1080-1088, https://doi.org/10.1016/j.biortech.2007.02.022.
7. Hu, Z.; Chen, H.; Ji, F.; Yuan, S. Removal of Congo Red from aqueous solution by cattail root. *Journal of Hazardous Materials* **2010**, *173*, 292-297, https://doi.org/10.1016/j.jhazmat.2009.08.082.
8. Cai, Z.; Sun, Y.; Liu, W.; Pan, F.; Sun, P.; Fu, J. An overview of nanomaterials applied for removing dyes from wastewater. *Environmental science and pollution research international* **2017**, *24*, 15882-15904, https://doi.org/10.1007/s11356-017-9003-8.
9. Wong, Y.C.; Szeto, Y.S.; Cheung, W.H.; McKay, G. Adsorption of acid dyes on chitosan—equilibrium isotherm analyses. *Process Biochemistry* **2004**, *39*, 695-704, https://doi.org/10.1016/S0032-9592(03)00152-3.
10. Guo, T.; Yao, M.; Lin, Y.H.; Nan, C.W. A comprehensive review on synthesis methods for transition-metal oxide nanostructures. *CrystEngComm* **2015**, *17*, 3551-3585, https://doi.org/10.1039/C5CE00034C.
11. Naika, H.R.; Lingaraju, K.; Manjunath, K.; Kumar, D.; Nagaraju, G.; Suresh, D.; Nagabhushana, H. Green synthesis of CuO nanoparticles using Gloriosa superba L. extract and their antibacterial activity. *Journal of Taibah University for Science* **2015**, *9*, 7-12, https://doi.org/10.1016/j.jtusci.2014.04.006.
12. Sutradhar, P.; Saha, M.; Maiti, D. Microwave synthesis of copper oxide nanoparticles using tea leaf and coffee powder extracts and its antibacterial activity. *Journal of Nanostructure in Chemistry* **2014**, *4*, https://doi.org/10.1007/s40097-014-0086-1.
13. Saranya, S.; Eswari, A.; Gayathri, E.; Eswari, S.; Vijayarani, K. Green Synthesis of Metallic Nanoparticles using Aqueous Plant Extract and their Antibacterial Activity. *International Journal of Current Microbiology and Applied Sciences* **2017**, *6*, 1834-1845, https://doi.org/10.20546/ijcmas.2017.606.214.
14. Naika, H.R.; Lingaraju, K.; Manjunath, K.; Kumar, D.; Nagaraju, G.; Suresh, D.; Nagabhushana, H. Green synthesis of CuO nanoparticles using Gloriosa superba L. extract and their antibacterial activity. *Journal of Taibah University for Science* **2015**, *9*, 7-12, https://doi.org/10.1016/j.jtusci.2014.04.006.
15. Ismail, M.; Gul, S.; Khan, M.I.; Khan, M.A.; Asiri, A.M.; Khan, S.B. Green synthesis of zerovalent copper nanoparticles for efficient reduction of toxic azo dyes congo red and methyl orange. *Green processing and synthesis* **2019**, 8(1), 135-143, https://doi.org/10.1515/gps-2018-0038.
16. Dil, E.A.; Ghaedi, M.; Asfaram, A. The performance of nanorods material as adsorbent for removal of azo dyes and heavy metal ions: Application of ultrasound wave, optimization and modeling. *Ultrasonics Sonochemistry* **2017**, *34*, 792-802, https://doi.org/10.1016/j.ultsonch.2016.07.015.
17. Saranya, S.; Eswari, A.; Gayathri, E.; Eswari, S.; Vijayarani, K. Green Synthesis of Metallic Nanoparticles using Aqueous Plant Extract and their Antibacterial Activity. *Int. J. Curr. Microbiol. App. Sci.* **2007**, *6*, 1834-1845, https://doi.org/10.20546/ijcmas.2017.606.214.
18. Asemani, M.; Anarjan, N. Green synthesis of copper oxide nanoparticles using Juglans regia leaf extract and assessment of their physico-chemical and biological properties. *Green Processing and Synthesis* .**2019** ,8(1) , 557-567, https://doi.org/10.1515/gps-2019-0025
19. Asghar, M.A.; Zahir, E.; Shahid, S.M.; Khan, M.N.; Asghar, M.A.; Iqbal, J.; Walker, G. Iron, copper and silver nanoparticles: Green synthesis using green and black tea leaves extracts and evaluation of antibacterial, antifungal and aflatoxin B1 adsorption activity. *LWT* **2018**, *90*, 98-107, https://doi.org/10.1016/j.lwt.2017.12.009.
20. Suárez-Cerda, J.; Espinoza-Gómez, H.; Alonso-Núñez, G.; Rivero, I.A.; Gochi-Ponce, Y.; Flores-López, L.Z. A green synthesis of copper nanoparticles using native cyclodextrins as stabilizing agents. *Journal of Saudi Chemical Society* **2017**, *21*, 341-348, https://doi.org/10.1016/j.jscs.2016.10.005.
21. Graham, H.N. Green tea composition, consumption, and polyphenol chemistry. *Preventive Medicine* **1992**, *21*, 334-350, https://doi.org/10.1016/0091-7435(92)90041-F.
22. Ali, I.; Peng, C.; Lin, D.; Naz, I. Green synthesis of the innovative super paramagnetic nanoparticles from the leaves extract of Fraxinus chinensis Roxb and their application for the

decolourisation of toxic dyes. *Green Processing and Synthesis* . **2019**,8(1) ,256-271, https://doi.org/10.1515/gps-2018-0078
23. Asl, M.; Mahmodi, N.; Teymouri, P.; Shahmoradi, B.; Rezaee, R.; Maleki, A. Adsorption of organic dyes using copper oxide nanoparticles: isotherm and kinetic studies. *Desalination and Water Treatment* **2016**, 1-10, https://doi.org/10.1080/19443994.2016.1151832.
24. Hussain, I.; Singh, N.B.; Singh, A.; Singh, H.; Singh, S. Green synthesis of nanoparticles and its potential application. *Biotechnology Letters* **2016**, *38*, 545-560, https://doi.org/10.1007/s10529-015-2026-7.
25. Gautam, P. K.; Shivalkar, S.; Samanta, S. K. Environmentally Benign Synthesis of Nanocatalysts: Recent Advancements and Applications: *Handbook of Nanomaterials and Nanocomposites for Energy and Environmental Applications* . Springer **2020**, 1-19. https://doi.org/10.1007/978-3-030-11155-7_52-1
26. Ghaedi, M.; Shojaeipour, E.; Ghaedi, A.M.; Sahraei, R. Isotherm and kinetics study of malachite green adsorption onto copper nanowires loaded on activated carbon: Artificial neural network modeling and genetic algorithm optimization. *Spectrochimica Acta Part A: Molecular and Biomolecular Spectroscopy* **2015**, *142*, 135-149, https://doi.org/10.1016/j.saa.2015.01.086.
27. Bushra, F.; Siddiqui, S.; Ahmed, R.; Chaudhry, S. A. Preparation of functionalized CuO nanoparticles using Brassica rapa leave extract for water purification. Mesalination and Water Treatment 2019, 164, 192-205. https://doi:10.5004/dwt.2019.24393
28. Divya, N.; Bansal, A.; Jana, A.K. Photocatalytic degradation of azo dye Orange II in aqueous solutions using copper-impregnated titania. *International Journal of Environmental Science and Technology* **2013**, *10*, 1265-1274, https://doi.org/10.1007/s13762-013-0238-8.
29. Zhang, P.; Hou, D.; O'Connor, D.; Li, X.; Pehkonen, S.; Varma, R.S.; Wang, X. Green and Size-Specific Synthesis of Stable Fe–Cu Oxides as Earth-Abundant Adsorbents for Malachite Green Removal. *ACS Sustainable Chemistry & Engineering* **2018**, *6*, 9229-9236, https://doi.org/10.1021/acssuschemeng.8b01547.
30. Ghaedi, M.; Zeinali, N.; Ghaedi, A.M.; Teimuori, M.; Tashkhourian, J. Artificial neural network-genetic algorithm based optimization for the adsorption of methylene blue and brilliant green from aqueous solution by graphite oxide nanoparticle. *Spectrochimica Acta Part A: Molecular and Biomolecular Spectroscopy* **2014**, *125*, 264-277, https://doi.org/10.1016/j.saa.2013.12.082.
31. Ghaedi, M.; Ghaedi, A.M.; Abdi, F.; Roosta, M.; Sahraei, R.; Daneshfar, A. Principal component analysis-artificial neural network and genetic algorithm optimization for removal of reactive orange 12 by copper sulfide nanoparticles-activated carbon. *Journal of Industrial and Engineering Chemistry* **2014**, *20*, 787-795, https://doi.org/10.1016/j.jiec.2013.06.008.
32. Ghaedi, M.; Ghaedi, A.M.; Negintaji, E.; Ansari, A.; Mohammadi, F. Artificial neural network – Imperialist competitive algorithm based optimization for removal of sunset yellow using $Zn(OH)_2$ nanoparticles-activated carbon. *Journal of Industrial and Engineering Chemistry* **2014**, *20*, 4332-4343, https://doi.org/10.1016/j.jiec.2014.01.041.
33. Ghaedi, M.; Ansari, A.; Assefi Nejad, P.; Ghaedi, A.; Vafaei, A.; Habibi, M.H. Artificial neural network and Bees Algorithm for removal of Eosin B using Cobalt Oxide Nanoparticle-activated carbon: Isotherm and Kinetics study. *Environmental Progress & Sustainable Energy* **2015**, *34*, 155-168, https://doi.org/10.1002/ep.11981.

6. ACKNOWLEDGEMENTS

The authors would like to thank all the technicians of the center of atomic science and physics department (CASP) at the Government College University (GCU), Lahore, Pakistan for providing SEM, XRD, FTIR facilities.